Original scientific paper

Colour prediction in multilayer polymer systems under polarized light for packaging applications

ABSTRACT

Conventional colour measurement methods do not fully account for the optical properties of multilayer polymer systems in transmitted polarized light. This work presents a Mueller-calculus-based model that predicts the spectral radiance and perceived colour of multilayer anisotropic polymer film stacks viewed in polarized light, targeting design needs in packaging. The model accepts the light source spectrum, polarizer and analyser angles, film optical-axis orientations, polymer film birefringence, and the spectral transmittance of added colour filters. The model was implemented in Python using SymPy and Colour libraries. Validation experiments employed stacks 1–3 layers at a 45-degree angle of 25±5 µm thickness BOPP films between parallel and crossed polarizers with a measured LED light source and X-Rite i1Pro spectrophotometer, including stacks combined with three gel colour filters and three flexographically printed patches on BOPP; BOPP birefringence was retrieved as Δn 0.015 via spectral analysis and it is consistent with the literature. The model reproduced key spectral features and colour coordinates, yielding absolute spectral RMSEs of 0.34-1.01 mW/(m²·sr·nm) for stacks without colour filters and a mean RMSE of 0.27 mW/(m²·sr·nm) with colour filters. The mean colour difference ΔE_{76} across configurations with colour filters was 10.8. The model can be used for preview prototyping of polarized-light effects and security features in multilayer packaging and may provide a basis for an intelligent colour-management system.

Vladislav Vereshchagin [1]
Aleksandra Pogiba [2]
Alexander Kondratov [2]

[1] Moscow Polytechnic University, Department of Incognitive Technologies, Moscow, Russia
[2] Moscow Polytechnic University, Department of Innovative Materials of Printmedia Industry, Moscow, Russia

Corresponding author:
Vladislav Vereshchagin
e-mail:
slavaver@ya.ru

First received: 25.9.2025.
Revised: 11.1.2026.
Accepted: 21.1.2026.

KEY WORDS
colorimetry, birefringence, Mueller calculus, packaging, polarized light, polypropylene, BOPP

Introduction

Control of colour and visual effects in modern packaging materials is of major commercial and scientific interest (Tomiša & Vusić, 2019). Among the key factors influencing these visual properties are the optical characteristics of the materials. Some polymer films are anisotropic materials and have different refractive indices along the optical axis and the transverse direction. As a result, two light beams propagate through such a material at different speeds (Samadi-Dooki et al., 2024). When light passes sequentially through a polarizer, a film sample, and an analyser, the analyser recombines the two beams. Since these beams travel at different speeds within the film, they acquire optical path difference determined by difference in refractive indexes and film thickness. Therefore, the transmitted light is no longer a mixture of colours forming white light, but a single interference colour, arising from the recombination of two waves. This optical property of anisotropic materials is known as birefringence. Birefringence is widely used in photoelasticity to analyse stress distribution in solids. Another application is the creation of colourful images under polarized light. The author termed such images PFC (polarization-filtered coloration) images (Slepkov, 2022a), generated using a different number of polymer film layers and orientations. This concept can, to some extent, be adapted for packaging applications.

Further use lies in anti-counterfeiting technologies. By stacking polymer films with anisotropic properties with cutouts in one or more layers, readable barcodes can be designed to appear only in polarized light (Kondratov et al., 2023). Moreover, biobased cellulosic materials with birefringence enable eco-friendly anti-counterfeiting solutions (Li et al., 2024).

Polymer films are widely used for packaging in multilayer systems, where the industry demands both colour constancy and predictability. The visual appearance of packaging plays an important role in successful marketing and design significantly affects respondents' decision-making process (Febriant, Widodo & Faizin, 2023; Malešević & Stančić, 2021).

Therefore, predicting the resulting colour effect is essential for utilizing birefringent polymer films in colourful packaging.

Quantitative analysis of interference colours observed in samples with double refraction (birefringence) is usually carried out using the Michel-Levy diagram. This method correlates interference colours, observed in optical microscopy or recorded digitally, with the sample's retardation, thickness, and birefringence (Linge Johnsen et al., 2018). The Michel–Lévy chart is generally applied when the optical axis of the sample is oriented at 45° to the polarizers.

The aim of this study was to develop a model for predicting the colours generated by multiple anisotropic polymer films with the addition of colourful layer viewed in polarized light, with practical applications in the packaging industry. The model accounts for the following known conditions: the spectral characteristic of the light source, the rotation angles of the polarizer and analyser, the orientation of the polymer film's optical axis, the film thickness, the induced phase shift (dependent on film thickness, refractive indices and light wavelength) and spectral transmittance of the colourful layer.

To our knowledge, the application of Mueller calculus for colour prediction in multilayer anisotropic polymer systems for packaging industry under controlled polarization conditions is novel.

The practical use of the developed model is prototyping anti-counterfeiting designs in multilayer polymer labels in packaging. It helps to create readable barcodes that become visible only under polarized light, eliminating the need to physically test various material combinations and layer configurations and reduces costly trial-and-error processes. Later, the model can be integrated into soft-proofing and ink formulation software systems. This integration would enable designers to combine interference colours generated by birefringent polymer layers with ink layers to achieve target colour specifications.

Model

Mueller calculus provides a mathematical formalism for describing the transformation of the polarization state of light as it interacts with various optical elements. It describes fully polarized, partially polarized, and unpolarized light, which are common in experimental and natural conditions. This suitability for complex systems, where multiple polarization effects occur simultaneously, provides predictive power for interpreting experimental measurements (Bass, 1995; del Toro Iniesta, 2003).

In this formalism, the polarization of an electromagnetic wave is represented by the four-component Stokes vector, which captures both the intensity and polarization characteristics of the beam. In this study, the unpolarized beam radiating from the light source was described by a series of special-case Stokes vectors $\overrightarrow{S_\lambda}$ for each wavelength λ (1).

$$\overrightarrow{S_\lambda} = \begin{bmatrix} I_\lambda \\ 0 \\ 0 \\ 0 \end{bmatrix} \tag{1}$$

where, I_λ is intensity of the light at a given wavelength.

The optical element is described by a 4x4 real-valued Mueller matrix that operates linearly on the Stokes vector, thereby enabling a unified treatment of a wide range of optical effects, including birefringence. There are Mueller matrixes for linear polarizers $M_P(\phi)$ (2), a general linear retarder $M_R(\delta, \theta)$ (3), a simple non-polarizing colour filter $M_F(\lambda)$ (4) for a given wavelength λ and neutral density filter. Colour filters were described by an identity matrix scaled by the filter's transmittance and neutral density filter is based on a simple non-polarizing colour filter but have same value T for all wavelengths λ.

$$M_P(\phi) = \begin{bmatrix} \frac{1}{2} & \frac{\cos(2\phi)}{2} & \frac{\sin(2\phi)}{2} & 0 \\ \frac{\cos(2\phi)}{2} & \frac{\cos(4\phi)}{4} + \frac{1}{4} & \frac{\sin(4\phi)}{4} & 0 \\ \frac{\sin(2\phi)}{2} & \frac{\sin(4\phi)}{4} & \frac{1}{4} - \frac{\cos(4\phi)}{4} & 0 \\ 0 & 0 & 0 & 0 \end{bmatrix} \tag{2}$$

where, ϕ is the angle of the transmission axis relative to the horizontal plane.

$$M_R(\delta,\theta) = \begin{bmatrix} 1 & 0 & 0 & 0 \\ 0 & \cos^2(2\theta) + \sin^2(2\theta)\cos\delta & \cos(2\theta)\sin(2\theta)(1-\cos\delta) & \sin(2\theta)\sin\delta \\ 0 & \cos(2\theta)\sin(2\theta)(1-\cos\delta) & \sin^2(2\theta) + \cos^2(2\theta)\cos\delta & -\cos(2\theta)\sin\delta \\ 0 & -\sin(2\theta)\sin\delta & \cos(2\theta)\sin\delta & \cos\delta \end{bmatrix} \tag{3}$$

where, δ is the phase difference between the fast and slow axes of the transmitted light and θ is the angle of the fast axis relative to the horizontal plane.

$$M_F(\lambda) = I_4 T(\lambda) \quad (4)$$

where, I_4 is a 4x4 identity matrix, λ is wavelength, T (λ) is transmittance for wavelength λ.

The resulting Stokes vector, $\overrightarrow{S_O}$ (5), is then calculated via matrix multiplication.

$$\overrightarrow{S_O} = M_N \cdots M_2 M_1 \overrightarrow{S_\lambda} \quad (5)$$

where, $\overrightarrow{S_\lambda}$ is Stokes vector for unpolarized light, $M_N \cdots M_2 M_1$ is optical element M_1 followed by M_2 and till M_N.

This model was implemented in a program written in Python. The main libraries that were used in implementation: Sympy (Meurer et al., 2017) and Colour (Mansencal et al., 2024). Code for this project can be found on the GitHub repository (https://github.com/slavaver/birefringence-model).

Materials and equipment

A series of optical experiments was conducted to validate the predictions of the developed model. Polymer film samples, polarizers, colour filters, a LED-light source with a diffuser and a spectrophotometer were employed. The experimental setup is shown in figure 1.

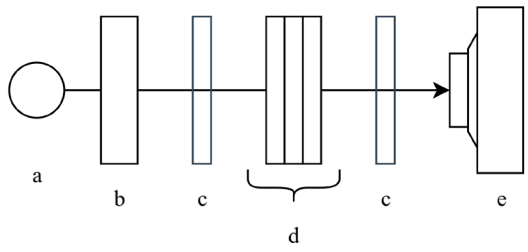

» **Figure 1:** *A diagram of the experimental setup used for taking spectral measurements, a – light source, b – diffusor, c – polarizer, d – stack of BOPP polymer films (1-3 layers), e – spectrophotometer*

All data were obtained with the spectrophotometer X-Rite i1Pro rev. D with spectral readings from 380 nm to 730 nm in 10 nm steps using ArgyllCMS utility “spotread” in emissive measurement mode (absolute results) resulting in spectral radiance in mW/(m²·sr·nm) data. Results represent single measurements only. The manufacturer's specification states short-term repeatability: x, y ±0.002 typ. (5000 K, 80 cd/m²). All measurements were conducted in a darkened room to eliminate ambient light interference. Spectrophotometer self-calibration was performed before measurements using the built-in white reference.

The X-Rite i1Pro was calibrated against the instrument's white reference standard (99% diffuse reflectance) in absolute radiance measurement mode. In one of the works authors used a similar spectrophotometer and have stated that relative standard deviations (RSD) of measurement vary from 0.1% to 1% (Apyari et al., 2011). In this case maximum relative expanded uncertainty for approximate 95% reference interval (RI) U(95%RI) = 2 × RSD = 2%.

The first component of the experimental setup is a LED-light source and a diffuser. Their measured spectral radiance (mW/(m²·sr·nm)) is shown in figure 2.

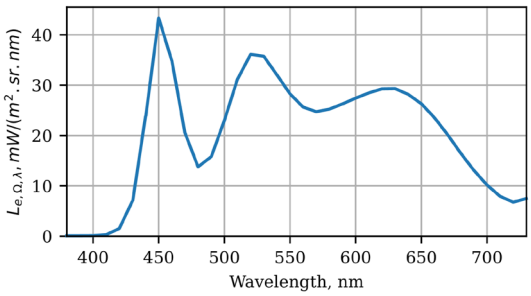

» **Figure 2:** *Measured spectral radiance in mW/(m²·sr·nm) of LED-lights emission after diffusor using spectrophotometer X-Rite i1Pro*

The linear polarizer from TAC and PVA declared characteristics are transmittance 0.41 when single and 0.05 when crossed (Fig. 3). Polarizing efficiency is 99.99%, wavelength range- 380~800nm, thickness- 0.25mm. To account for the difference between an ideal polarizer (transmittance 0.50) and the real polarizer used (transmittance 0.41), an additional coefficient of 0.82 was applied.

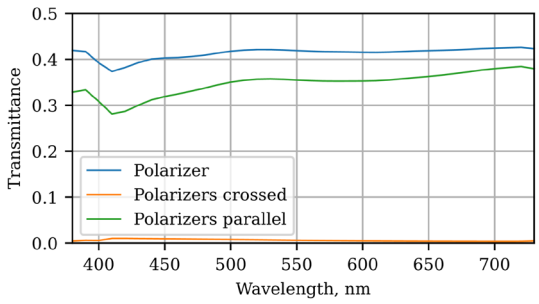

» **Figure 3:** *Spectral transmittance of one polariser and two polarisers with parallel and crossed transmission axes to compare declared and real transmittance*

Biaxially oriented isotactic polypropylene (BOPP) films with a thickness of 25±5 µm were used in experiments.

The mean spectral transmittance of 1 layer of BOPP film is 0.99. The birefringence of the BOPP film was obtained with spectral content analysis (SCA) method measuring spectral transmittance with crossed and parallel

polarizers, but a costly polarimetric gate was replaced with the experimental setup using an X-Rite i1Pro (Slepkov, 2022b; Ajovalasit, Barone & Petrucci, 1998).

The retardance Γ produced by the birefringent sample depends on the distance d travelled by the light of wavelength λ in the sample (6).

From the literature it is known that under certain wavelength material can behave like a half-wave plate and this leads to the biggest difference in transmittance between parallel and crossed polarizers. One and two layers of BOPP films were used and two layers showed more visible difference in transmittance (Fig. 4) and based on the characteristics of film retardance is equal to 0.015.

$$\Gamma = \frac{2\pi\Delta n d}{\lambda} \tag{6}$$

where, Γ – retardance, Δn – birefringence,
d – material thickness, λ – wavelength.

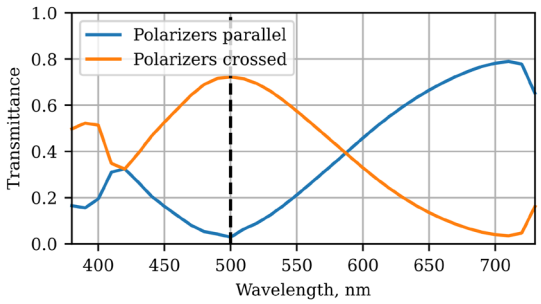

» **Figure 4:** *Spectral transmittance of two layers of BOPP films 25 µm between polarizers in parallel and crossed configurations. Polymer films oriented with their optical axis at 45° to the transmission axis of the input polarizer. Vertical dashed line at 500 nm marks where stack acts as half-wave plate*

Calculated birefringence matches with values in "Guideline for Using Light Microscopy in Forensic Examinations of Tape Components Scientific Working Group for Materials Analysis" in the range of 0.014- 0.016 and value in Table I of the article (Slepkov, 2022b).

Three gel colour filters red, green and blue were used in the experiment. Their spectral transmittance shown in figure 4.

These filters don't exhibit anisotropic properties as they don't show colour change in different angle between two polarisers. The other three filters are an ink layer on BOPP films of yellow, cyan and magenta colours printed by flexographic method (Fig. 5).

In the model they account as two optical elements one film layer and one colour filter.

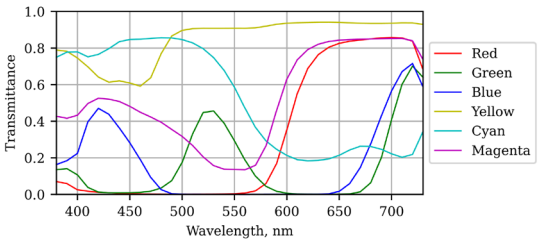

» **Figure 5:** *Spectral transmittance of gel colour filters (red, green, blue) and yellow, cyan, magenta colour patches on BOPP films 25 µm used in experiment*

Results

On this step the developed model was validated using stacks of BOPP films (25 µm thickness) 1-3 layers without additional colour layers in crossed and parallel polarizers. Stacks of BOPP films were oriented with their optical axis at 45° to the transmission axis of the input polarizer.

A comparison of the modelled and experimental spectral radiance is shown in Figure 6 and absolute root mean square errors (RMSE) values for the spectral radiance ranges from 0.34 to 1.01 for different layer configurations and polarizer orientations (Table 1). Maximum relative error is approximately 10%.

Table 1

Comparison of absolute RMSE in mW/(m²·sr·nm) between experimental and calculated spectral radiance for stacks of BOPP films with number of layers from 1 to 3 in parallel and crossed polarizers. Stacks of BOPP films were oriented with their optical axis at 45° to the transmission axis of the input polarizer

Layers	Polarizers	RMSE
1	Parallel	0.34
2		0.57
3		1.01
1	Crossed	0.50
2		0.66
3		0.95

The chromaticity diagram (Figure 7) illustrates the colour coordinates of samples with a varying number of BOPP layers under crossed and parallel polarizer configurations.

The experimental data points (circles) and model predictions (triangles) show reasonable correlation, particularly for single and double-layer configurations.

Colour difference ΔE_{76} in the CIELab colour space revealed values ranging from 3.2 to 22.5 between experimental and calculated data (Table 2).

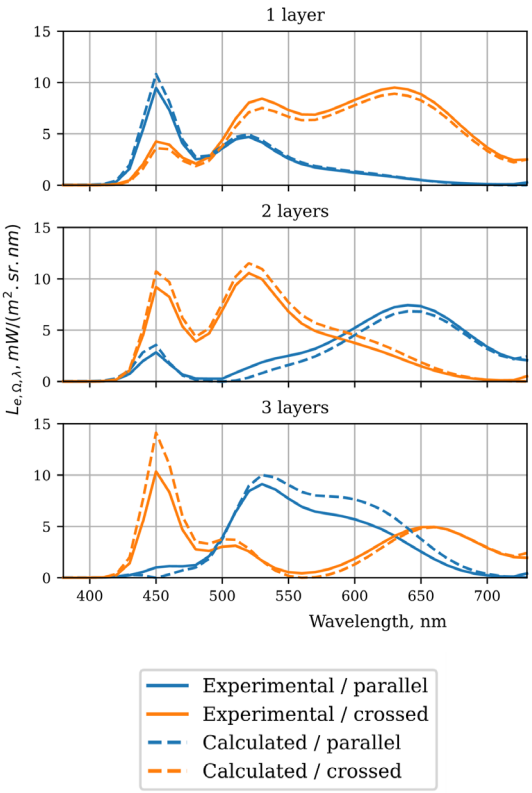

» **Figure 6:** *Spectral radiance comparison between experimental and calculated with the developed model for stacks of BOPP films with number of layers from 1 to 3 (25 µm per layer) under parallel and crossed linear polarizer configuration. Stacks of BOPP films were oriented with their optical axis at 45° to the transmission axis of the input polarizer*

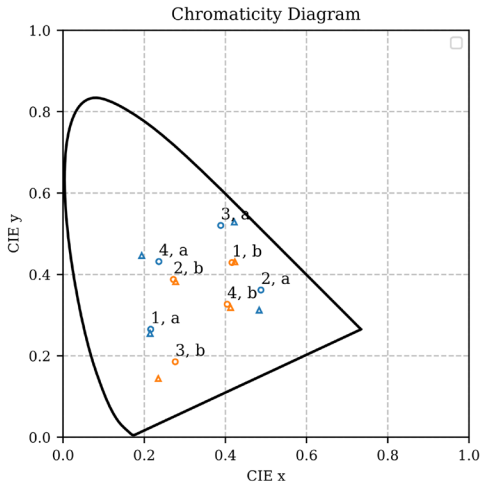

» **Figure 7:** *Chromaticity diagram with colours for 1-3 layer BOPP stacks (25 µm per layer) under parallel and crossed linear polarizer configuration. Stacks of BOPP films were oriented with their optical axis at 45° to the transmission axis of the input polarizer. Number on diagram specifies number of layers of BOPP, letter a is for parallel polarizers and b for crossed. Circles are for experimental data and triangles – calculated data*

The model showed agreement with experimental observations in reproducing the spectral features and overall radiance patterns. The lowest deviations were observed for single-layer samples, while increasing complexity with additional layers resulted in higher error values.

The model was also validated using stacks that included colour layers in crossed and parallel polarizers and stacks were placed at a 45° angle. Six different colour filters: yellow, cyan, magenta, red, green, and blue were tested in combination with 1-3 layers of BOPP films. Examples of two cases with green and cyan colour filters shown in Figure 8. They demonstrate the model's capability to predict the spectral shape and magnitude. The calculated data follow the experimental curves, capturing the characteristic features of the interference patterns.

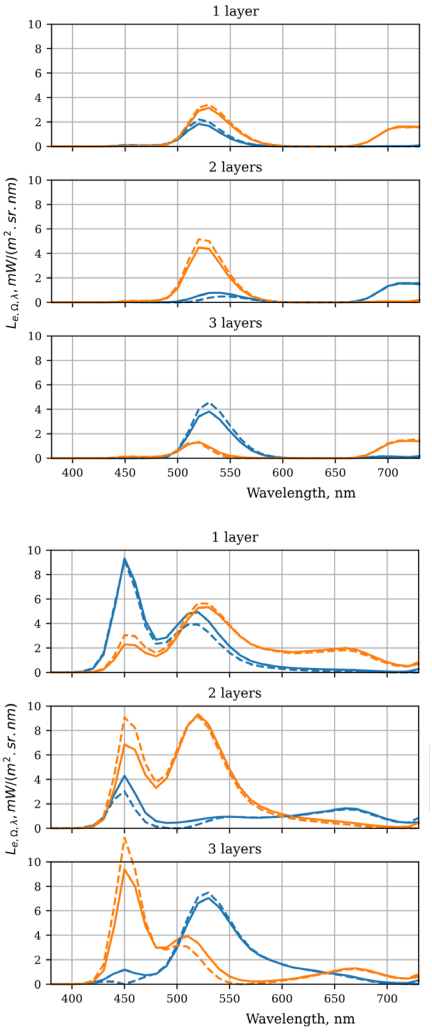

» **Figure 8:** *Spectral radiance comparison between experimental and calculated with the developed model for stacks of BOPP films with number of layers from 1 to 3 (25 µm per layer) under parallel and crossed linear polarizer configuration and green colour filter on the left and cyan filter on the right. Stacks of BOPP films were oriented with their optical axis at 45° to the transmission axis of the input polarizer*

Table 2

Comparison of CIELab coordinates for resulting colours for 1-3 layer BOPP stacks (25 µm per layer) under parallel and crossed linear polarizer configuration. Stacks of BOPP films were oriented with their optical axis at 45° to the transmission axis of the input polarizer and colour difference ΔE_{76} between experimental and calculated data

Layers	Polarizers	Experimental			Calculated			ΔE_{76}
		L	a	b	L	a	b	
1	Parallel	48.9	-14.0	-24.1	50.3	-11.5	-27.5	4.5
2		54.8	37.7	33.4	48.7	49.2	17.4	20.7
3		73.0	-29.7	70.0	78.3	-23.1	90.8	22.5
1	Crossed	77.4	2.7	49.7	74.7	4.3	50.5	3.2
2		71.3	-36.3	10.4	75.1	-33.9	10.3	4.5
3		42.1	40.5	-38.7	40.2	47.4	-56.3	19.0

The mean absolute RMSE across all configurations was 0.27. Table 3 shows the absolute RMSE values for each colour filter and layer combination. The relative error is approximately 10%.

The colour prediction accuracy was evaluated using ΔE_{76} values in the CIELab colour space.

Table 3

Comparison of absolute RMSE in mW/(m²·sr·nm) between experimental and calculated spectral radiance for stacks of BOPP films with number of layers from 1 to 3 in parallel and crossed polarizers and yellow, cyan, magenta, red, green and blue colour filters. Stacks of BOPP films were oriented with their optical axis at 45° to the transmission axis of the input polarizer

Layers	Polarizers	RMSE						
		Yellow	Cyan	Magenta	Red	Green	Blue	Mean
1	Parallel	0.28	0.37	0.23	0.02	0.11	0.10	0.19
2		0.52	0.38	0.45	0.15	0.12	0.05	0.28
3		0.67	0.30	0.39	0.30	0.22	0.06	0.32
1	Crossed	0.35	0.25	0.34	0.10	0.09	0.06	0.20
2		0.44	0.57	0.15	0.17	0.20	0.13	0.28
3		0.58	0.67	0.41	0.17	0.07	0.33	0.37
Mean		0.47	0.42	0.33	0.15	0.13	0.12	**0.27**

The overall mean colour difference across all tested configurations was 10.8 (Table 4).

Single-layer samples with crossed polarizers achieved the best performance (mean $\Delta E_{76} = 3.8$), approaching the threshold for acceptable colour matching in many industrial applications.

Table 4

Comparison of colour difference ΔE_{76} for resulting colours for 1-3 layer BOPP stacks (25 µm per layer) under parallel and crossed linear polarizer configuration and 6 colour filters. Stacks of BOPP films were oriented with their optical axis at 45° to the transmission axis of the input polarizer. Mean values for each filter and layer combination are presented

Layers	Polarizers	ΔE_{76}						
		Yellow	Cyan	Magenta	Red	Green	Blue	Mean
1	Parallel	3.0	12.2	7.3	0.8	6.5	9.3	6.5
2		16.5	9.6	12.4	3.8	20.7	6.5	11.6
3		19.1	17.1	24.1	9.1	9.4	23.5	17.0
1	Crossed	2.2	6.9	4.8	0.5	3.8	4.9	3.8
2		4.0	13.2	2.9	6.8	7.0	9.4	7.2
3		20.0	35.8	18.3	3.1	8.8	24.0	18.3
Mean		10.8	15.8	11.6	4.0	9.4	12.9	**10.8**

The performance of the model can be contextualized using standard ΔE_{76} thresholds from colorimetry literature ΔE_{76} 2-4 is noticeable to most observers; and $\Delta E_{76} > 4$ represents clear colour differences.

Discussion

The experimentally determined birefringence Δn of 0.015 for the BOPP films aligns well with published literature values. This result confirms the reliability of the measurement method, which utilizes a spectrophotometer commonly employed in the printing industry.

The model using Mueller calculus demonstrates predictive capability. With a mean absolute RMSE of 0.27 and mean colour difference ΔE_{76} of 10.8, the model's performance is sufficient for preview applications in packaging design. However, for critical colour matching applications requiring ΔE_{76} lower than 4, further optimization of the model is necessary.

A trend of decreasing accuracy was observed as the number of film layers increased. This can likely be attributed to the cumulative optical effects and increased complexity of interference patterns within multilayer systems. Single-layer samples under crossed polarizers showed the best ΔE_{76} of 3.8, while three-layer samples under parallel polarizers exhibited the largest difference ΔE_{76} of 18.3.

The model uses film thickness (d) as an explicit parameter in the phase retardance calculation (Equation 6). This allows accommodation of manufacturing thickness variations. However, the current measurement aperture of the used spectrophotometer is 4.5 mm and model validation reflects the averaged optical properties on plane. Direct comparison between model predictions and real BOPP films with spatially varying thickness requires an understanding of the rate of thickness change.

Future work should address several areas for model improvement. These include:
(1) investigating the effects of non-normal light incidence; (2) integrating the ink spectral collection system proposed by (Zhang et al., 2024); and (3) exploring neural network approaches to account for potential non-linear optical effects and improve predictive accuracy.

Conclusion

In this study, a Mueller calculus-based model was developed and validated for predicting the colour of multilayer BOPP systems. The model can predict spectral radiance and resultant colour for multilayer BOPP stacks under polarized light conditions with accuracy of an absolute mean RMSE of 0.27 mW/(m^2·sr·nm) for spectral composition predictions and colour differences with mean ΔE_{76} of 10.8 across six chromatic filters.

While the theoretical framework is material-agnostic, all experimental validation and colour accuracy benchmarking reported herein are specific to BOPP films with 25 µm thickness.

This study demonstrates that birefringence in BOPP films can be determined using a standard spectrophotometer, thereby avoiding the need for a more costly polarimetric gate. The experimentally derived BOPP birefringence Δn of 0.015 is consistent with literature values for transparent films, indicating that the retrieval pipeline is physically grounded for anisotropic polymer films used for packaging.

The proposed model provides a practical basis for an intelligent colour-management system. Such a system would enable virtual prototyping of multilayer stacks under various conditions, reducing trial-and-error in product design and facilitating the development of security features visible only under polarized light.

While the current model shows promising results for BOPP films, future work should explore its applicability to other common packaging materials, such as PET and PE, and investigate the influence of different polymer orientation states.

Funding

This work was financially supported by the Moscow Polytechnic University within the framework of the grant named after Vladimir Fortov.

References

Ajovalasit, A., Barone, S. & Petrucci, G. (1998) A review of automated methods for the collection and analysis of photoelastic data. *The Journal of Strain Analysis for Engineering Design.* 33 (2), 75–91. Available from: doi: 10.1243/0309324981512832

Apyari, V. V., Dmitrienko, S. G., Batov, I. V. & Zolotov, Y. A. (2011) An Eye-One Pro mini-spectrophotometer as an alternative to diffuse reflectance spectrometer. *Journal of Analytical Chemistry.* 66 (2), 144–150. Available from: doi: 10.1134/S1061934811020043

Bass, M. (1995) *Handbook of optics*. 2nd ed. New York, McGraw-Hill.

Febriant, I. A., Widodo, A. S. & Faizin, A. (2023) The effectiveness of Canned Coffee packaging's graphic design elements in consumers' decision-making process. *Journal of Graphic Engineering and Design.* 14 (4), 5–12. Available from: doi: 10.24867/JGED-2023-4-005

Kondratov, A. P., Nikolaev, A. A., Nazarov, V. G., Vereshchagin, V. Y. & Volinsky, A. A. (2023) Design and multilevel structuring of shape memory polymers for pleochroism control. *Journal of Applied Polymer Science.* 140 (41). Available from: doi: 10.1002/app.54532

Li, X., Qiu, X., Yang, X., Zhou, P., Guo, Q. & Zhang, X. (2024) Multi-Modal Melt-Processing of Birefringent Cellulosic Materials for Eco-Friendly Anti-Counterfeiting. *Advanced Materials.* 36 (36). Available from: doi: 10.1002/adma.202407170

Linge Johnsen, S., Bollmann, J., Lee, H. & Zhou, Y. (2018) Accurate representation of interference colours (Michel–Lévy chart): from rendering to image colour correction. *Journal of Microscopy.* 269 (3), 321–337. Available from: doi: 10.1111/jmi.12641

Malešević, M. & Stančić, M. (2021) Influence of packaging design parameters on customers' decision-making process. *Journal of Graphic Engineering and Design.* 12 (4), 33–38. Available from: doi: 10.24867/JGED-2021-4-033

Mansencal, T., Mauderer, M., Parsons, M., Shaw, N., Wheatley, K., Cooper, S., Vandenberg, J. D., Canavan, L., Crowson, K., Lev, O., Leinweber, K., Sharma, S., Sobotka, T. J., Moritz, D., Pppp, M., Rane, C., Eswaramoorthy, P., Mertic, J., Pearlstine, B., Leonhardt, M., Niemitalo, O., Szymanski, M., Schambach, M., Huang, S., Wei, M., Joywardhan, N., Wagih, O., Redman, P., Goldstone, J., Hill, S., Smith, J., Savoir, F., Saxena, G., Chopra, S., Sibiryakov, I., Gates, T., Pal, G., Tessore, N., Pierre, A., Thomas, F.-X., Srinivasan, S., Downs, T., Rusching, K., Chen, X., Herb, B., Caswell, T. A., Collod, L. & Brummer, B. (2024) *Colour 0.4.6* [Software]. Available from: doi: 10.5281/zenodo.13917514

Meurer, A., Smith, C. P., Paprocki, M., Čertík, O., Kirpichev, S. B., Rocklin, M., Kumar, A., Ivanov, S., Moore, J. K., Singh, S., Rathnayake, T., Vig, S., Granger, B. E., Muller, R. P., Bonazzi, F., Gupta, H., Vats, S., Johansson, F., Pedregosa, F., Curry, M. J., Terrel, A. R., Roučka, Š., Saboo, A., Fernando, I., Kulal, S., Cimrman, R. & Scopatz, A. (2017) SymPy: symbolic computing in Python. *PeerJ Computer Science.* 3, e103. Available from: doi: 10.7717/peerj-cs.103

Samadi-Dooki, A., Lamontia, M. A., Londoño, J. D., Williamson, C., Burch, H. E., Yahyazadehfar, M., Carbajal, L. A. & Kourtakis, K. (2024) Effect of Chain Orientation on Coupling of Optical and Mechanical Anisotropies of Polymer Films. *Coatings.* 14 (6), 764. Available from: doi: 10.3390/coatings14060764

Slepkov, A. D. (2022a) Painting in polarization. *American Journal of Physics.* 90 (8), 617–624. Available from: doi: 10.1119/5.0087800

Slepkov, A. D. (2022b) Quantitative measurement of birefringence in transparent films across the visible spectrum. *American Journal of Physics.* 90 (8), 625–634. Available from: doi: 10.1119/5.0087798

Tomiša, M. & Vusić, D. (2019) Deviations of Spot Colorimetric Values on Multi-layered Flexible Packaging during the Graphic Reproduction and Sterilisation Process. *Technical Gazette.* 26 (2). Available from: doi: 10.17559/TV-20190119234822

del Toro Iniesta, J. C. (2003) *Introduction to Spectropolarimetry*. Cambridge, Cambridge University Press. Available from: doi: 10.1017/cbo9780511536250

Zhang, W., Liu, X., Zhang, R., Jiang, F., He, J. & Fang, S. (2024) Design of printing ink spectral collection system and research on ink proportion prediction method. *AIP Advances.* 14 (4). Available from: doi: 10.1063/5.0186340